Full Convolutional Neural Network with Multi-Scale Residual Model for Optic Cup and Disc Segmentation

Yanxia Sun[1], Peiqing Lv[2], Xiaoxu Geng[3], Haiying Wang[2], Jinke Wang[1,4,*], and Shinichi Tamura[4]

[1]*Department of Software Engineering, Rongcheng College, Harbin University of Science and Technology, Rongcheng, 264300, China*
[2]*School of Automation, Harbin University of Science and Technology, Harbin, 150080, China*
[3]*School of Computer Science and Technology, Harbin University of Science and Technology, Harbin, 150080, China*
[4]*Center for Advanced Medical Engineering and Informatics, Osaka University, Suita, Japan, 565-0871, Japan*

Accurate optic cup and optic disc (OC, OD) segmentation is the prerequisite for cup-disc ratio (CDR) calculation. In this paper, a new full convolutional neural network (FCN) with multi-scale residual module is proposed. Firstly, polar coordinate transformation was introduced to balance the CDR with space constraints, and CLAHE was implemented in fundus images for contrast enhancement. Secondly, W-Net-R model was proposed as the main framework, while the standard convolution unit was replaced by the multi-scale residual module. Finally, the multi-label cost function is utilized to guide its functioning. In the experiment, the REFUGE dataset was used for training, validation and testing. We obtained 0.979 and 0.904 for OD and OC segmentations on MIoU, which indicates a relative improvement of 4.04% and 3.55%, comparing with that of U-Net, respectively. Experiment results proved that our proposed method is superior to other state-of-the-art schemes on OC and OD segmentation, and could be a potential prospective tool for early screening of glaucoma.

Keywords: FCN, OD, OC, Segmentation, Multi-Scale Residual Model, Glaucoma.

1. INTRODUCTION

Glaucoma blindness ranks second among various causes [1]. Since glaucoma-induced vision damage cannot be reversed, early diagnosis of glaucoma is crucial. However, manual annotation by doctors is time-consuming and subjective. Recent methods for glaucoma diagnosis are mainly binary-based classification with the optic nerve head in the fundus image [2]. Because larger Cup-Disc Ratio (CDR) value indicates greater risk of glaucoma, so accurate segmentations of Optic Cup (OC) and Optic Disc (OD) become keys of CDR evaluating. For segmentation of OD and OC, a variety of features are utilized, including color, texture, threshold, edge, and region, et al. [3–7]. However, these approaches are prone to be affected by poor quality of fundus images, which could lead to lower accuracies.

To improve the efficiency of feature extraction, some strategies were proposed based on the reduction of pixels number, e.g., superpixel-based method [8]. However, such method depends on manually designed features, which tend to result in poor reproducibility.

Under the premise of high processing performance, deep learning methods have overcome the limitations of manually designing features, and provides with highly distinguishable feature representations. For medical image segmentation, early deep learning methods were mostly based on image blocks [9], but sliding windows could cause redundant calculations and global information are failed to obtain. As end-to-end deep learning rises, FCN-based approaches quickly gained popularity in image classification and segmentation [10]. In which, the U-Net [11] has become a famous structure for medical image segmentation, while its improved models (such as M-Net [12], U-Net++ [13], MultiResUNet [14], Siam-U-Net [15]) also achieved fairly good performances on medical image segmentation.

As to OD and OC segmentation, many existing methods ignored the prior related knowledge between OD and OC, e.g., segment OD and OC separately [3–5, 16]. In such methods, each pixel corresponds to only one label (i.e., OC, OD, or background), which cuts off the connection between OD and OC. Although the current FCN-based models [10–15] are able to capture quite a few advanced features in the encoder, while retaining a considerable amount of spatial information in the decoder, there is still room for improvement in terms of the depth and width for the network learning.

In order to solve problems mentioned above, a new W-Net-R network structure for hybrid segmentation of OC and OD proposed in this paper. Compared with other FCNs, W-Net-R uses a

---

*Author to whom correspondence should be addressed.

W-type FCN as the main frame, which deepens the depth of the network and facilitates deep information learning. At the same time, this paper also proposes a multi-scale residual convolution learning module to replace the standard convolution learning unit in U-Net, which deepens the network width, so that it can capture more information at different scales in a limited scale range.

In the flowing sections, firstly, the proposed method is depicted in detail. Secondly, comparative experiments and discussions are provided. Finally, we gave conclusion of the proposed method.

2. METHOD

2.1. Image Preprocessing

2.1.1. Polar Coordinate Transformation

First, the automatic OD detection method proposed by Ref. [17] is utilized for center locating. Then, the disc area is segmented according to the specified pixel size to obtain the ROI. At last, pixel-level polar coordinate transformation is implemented, which maps the fundus images (Fig. 1(a)) to polar coordinates. The transformation relationship is as follows:

$$\begin{cases} r = \sqrt{u^2 + v^2} \\ \theta = \tan^{-1} v/u \end{cases} \tag{1}$$

where μ, ν represents the horizontal and vertical coordinates of a pixel in Cartesian coordinate system. θ, r represents the orientation angle and radius of a pixel in polar coordinates. As shown in the Figure 1(c), by polar transformation the ratio of OC area turns to be much higher than the ROI [12] (Fig. 1(b)), which can effectively improve the CDR, and prevent overfitting.

2.1.2. Data Enhancement

Since the number of fundus images is limited in the dataset, after obtaining the ROI and polar coordinate transformation, dataset enhancement is implemented to prevent overfitting. Random image transforming process is utilized, including random flips of horizontal, vertical, and diagonal, color dithering in HSV color space, and random image movement. By this way, the data augmentation process could be further enhanced via various random transforming operations, which helps improve the generalization performance.

2.1.3. Normalized Processing

The fundus image could have problems of uneven illumination and low contrast, which may affect glaucoma diagnosis. To increase the contrast between OC, OD and the background, CLAHE [18] is utilized (see Fig. 1(d)) for contrast enhancement and color normalization. By this way, uneven illumination and

low contrast are improved. Finally, the pre- and post-processing images are combined to construct the new channel images, making them more suitable for distinguishable features learning. In the same way, the polar coordinates of the label are transformed (as shown in Figs. 1(e–g)).

2.2. Framework Overview

The model framework proposed in this paper consists of 4 parts (shown in Fig. 2).

(i) The first part is a layer with multi-scale, used for building the input of the image pyramid and realize the input of original semantic information of different scales and optical properties, thereby greatly enriching the semantic information.

(ii) The second part is a W-type convolutional neural network, which is used as the main structure for learning different levels of features in the image.

(iii) The third part is to implement deep monitoring at the multi-sided output layers of different network depths, so that the gradient information is properly transmitted to the previous layer, which effectively suppresses the disappearance of the gradient, and is beneficial to the early training and learning of the network. In addition, a multi-scale full convolution module with residuals is proposed to extract more distinguishable features under different scales of receptive fields.

(iv) The fourth part is cost function with multi-label, which is utilized to guide hybrid segmentations of OD and OC.

2.2.1. Main Network Structure

The main network W-Net-R consists of two U-Nets. The former provides a shallower semantic expression to retain the original structural information to the greatest extent, while the latter is a further semantic abstraction for more abstract structural information. This structure deepens the depth of the nerves, so that the network can learn more deep structural information and more abstract semantic information. Coupled with skip connection, it can achieve semantic fusion of different depths on the same network scale, and guide the network to extract deeper distinguishable semantic representations.

Each encoding path performs convolution operation with convolution kernel to create a series of encoder feature mappings and the decoder feature images. Then, feature representation output of high dimension from the last decoder layer is input into a trainable classifier with multi-label, which uses a convolutional layer and the Sigmoid activation function to generate the prediction probability mapping to complete pixel level classifying. For the multi-label segmentations of OD and OC of this paper, the output is a probability prediction map of three channels, e.g., OD, OC, and background, respectively.
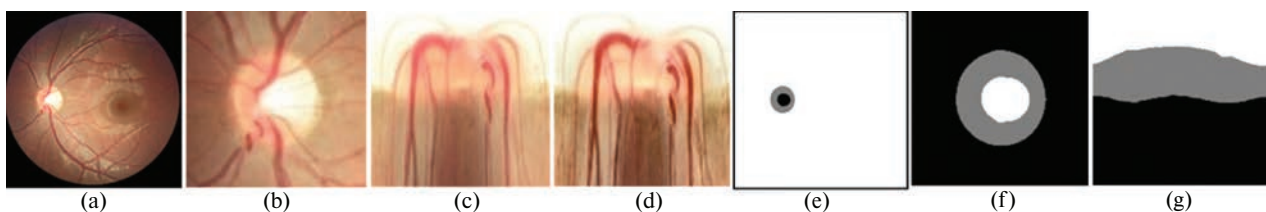
Fig. 1. Image preprocessing. (a) Original image. (b) ROI. (c) Polar coordinate transformation. (d) CLAHE. (e) Label. (f) Label ROI. (g) Label polar coordinate transformation.
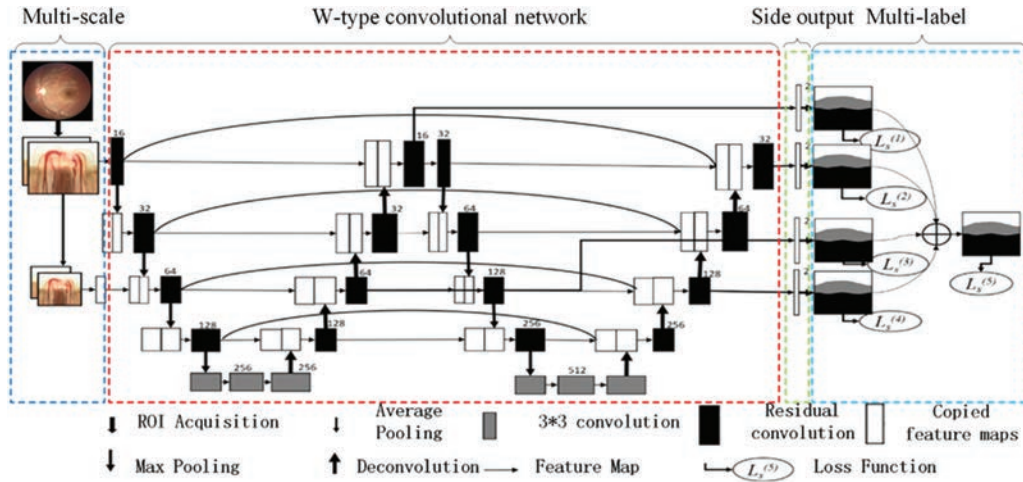
Fig. 2. Framework of W-Net-R model.

2.2.2. Multi-Scale Input Layer

Average pooling is utilized for downsampling the images, while building multi-scale inputs of encoding path. In this way, multi-scale inputs can be integrated into the coding layer, and avoid the increasement of the parameter and the width of the encoding path. In this paper, only one down-sampling process is performed to achieve a balance between the network depth and redundant input information.

2.2.3. Prophase Output Layer

In this paper, prophase output layer selects some channels of different depths, maintaining the same structure as the multi-scale output layer. By this way to reduce redundant information and monitor the network. The objective function that weighting the different prophase output layers is as follows,

$$\sigma_s = \sum_{n=0}^{N} \alpha_n L_s{}^{(n)} \tag{2}$$

in which, α_0 represents the fusion weight of the loss function of n-th prophase output layer, $L_s(n)$ denotes the multi-label cost of the n-th prophase output layer of the network, while N denotes the number of prophase output layers.

2.2.4. Multi-Label Loss Function

Hybrid OD and OC segmentation is an issue of multi-label. Unlike the pre-existing segmenting approaches, which uniquely label each instance according to a certain rule, by using multi-label approach, an instance can belong to multiple categories at the same time, which can effectively alleviate the imbalanced problem between OD and the background. In this step, a multi-label cost function is proposed, which are based on both Dice coefficient [19] and Focal-Loss [20]. Dice cost function Eq. (3) denotes the ratio of foreground mask overlap, which is used to handle the imbalance of foreground pixels and background. While Focal-Loss function Eq. (4) is utilized for solving the imbalance problems of dataset, because it is good at dealing with small sample areas that are difficult to segment. Their functions are as follows,

$$L_D = -\sum_{k}^{K} \frac{2\sum_{i}^{N} p_i g_i + \varepsilon}{\sum_{i}^{N} p_i^2 + \sum_{i}^{N} g_i^2 + \varepsilon} \tag{3}$$

$$L_F = \sum_{k}^{K} [-\alpha g_i (1-p_i)^\gamma \log(p_i) - \alpha(1-g_i)p_i{}^\gamma \log(1-p_i)] \tag{4}$$

$$L_s = L_D + L_F \tag{5}$$

where g_i and p_i denote the ground truth and the estimated probability for the i-the pixel; ε, α, γ are constant coefficients.

2.2.5. Residual Convolution Module

Inspired by the *Inception*-ResNet [21], we propose a residual convolution module to extract high-level semantic feature. Different from Inception-ResNet, in the residual convolution module, we use two 3×3 convolution units instead of 5×5, and use 1×7 and 7×1 modules instead of 7×7, which results in less parameters while maintain larger receptive field. In addition to performing feature mapping through four convolutional channels, the proposed framework also introduces a skip connection similar to ResNet [22], and by utilizing a standard 3×3 and 1×1 convolution units to perform dimensionality reduction and nonlinear activation. Finally, the obtained convolution units are skip connected with the input features to achieve the fusion of different depth features.

2.3. Evaluating Metric

For evaluating the segmentation performances of our proposed W-Net, 5 evaluation metrics were introduced, which have been commonly used to evaluate the accuracies of OD and OC segmentations, including 5 evaluation metrics are introduced. They include PA (Pixel Accuracy, MIoU (Mean Intersection over Union), FWIoU (Frequency Weighted Intersection over Union), and OE (Overlap Error) [23] Eqs. (6)–(10):

$$\text{PA} = \frac{\sum_i n_{ii}}{t} \tag{6}$$

$$\text{MA} = \frac{1}{n_{cl}} \sum_i \frac{n_{ii}}{t_i} \tag{7}$$

$$\text{MIoU} = \frac{1}{n_{cl}} \sum_i \frac{n_{ii}}{t_i + \sum_j n_{ji} - n_{ii}} \tag{8}$$

$$\text{FWIoU} = \frac{1}{t} \sum_i \frac{t_i n_{ii}}{t_i + \sum_j n_{ji} - n_{ii}} \tag{9}$$

$$\text{OE} = 1 - \sum_i \frac{n_{ii}}{t_i + \sum_j n_{ji} - n_{ii}} \tag{10}$$

Table I. Comparison for OC and OD segmentations among 6 models.

Models	OD					OC				
	OE	ACC	MA	MIoU	FWIoU	OE	ACC	MA	MIoU	FWIoU
U-Net	0.088	0.977	0.972	0.941	0.957	0.236	0.983	0.910	0.873	0.967
M-Net	0.082	0.981	0.975	0.943	0.960	0.196	0.985	0.938	0.897	0.973
W-Net	0.080	0.982	0.975	0.946	0.961	0.191	0.986	0.940	0.900	0.974
U-Net-R	0.078	0.980	0.972	0.948	0.961	0.217	0.984	0.927	0.883	0.970
M-Net-R	0.077	0.980	0.975	0.948	0.961	0.192	0.986	0.939	0.898	0.974
W-Net-R	0.066	0.984	0.979	0.956	0.968	0.178	0.987	0.950	0.904	0.976

where n_{cl} denotes the categories number, $t = \sum_i t_i$ represents the pixels number, $t_i = \sum_i n_{ij}$ denotes the total number of pixels belonging to i category, n_{ji} denotes the number of pixels whose ground truth is i, but is misclassified into j.

3. EXPERIMENT RESULT

3.1. Datasets

The REFUGE (REtinal FUndus Glaucoma ChallengE dataset (https://refuge.grand-challenge.org/) was utilized for verification, which is annotated as glaucoma and non-glaucoma. Each fundus image records 3 types of information: diagnostic, segmentation, and localization. All the images are Positioning center on posterior pole, containing both OD and macula. The dataset consists of 3 parts: training, testing and validating sets. For training dataset, 400 fundus images with resolution 2142×2056 were taken by Zeiss Visucam 500 fundus camera. For verification and testing datasets, each consists of 400 fundus images with resolution 1634×1634, taken by Canon CR-2 fundus camera. The experiments are implemented using Python and Tensorflow under Ubuntu 18.04, with Nvidia GeForce 2080Ti and Xeon Silver 4110 CPU. 600 fundus images for the training, 100 sets for verification, and 100 sets for the test. Experimental results are compared with ground truth annotated by seven experts.

3.2. Result and Discussion

We compared our proposed method with state-of-the-art ones, U-Net [11] and M-Net [12]. For verifying the superiority of our proposed approach, both M-Net and U-Net are used as the main frame, while the convolution unit is replaced by the residual multiscale convolution, named U-Net-R, M-Net-R respectively. Then, they are both compared with W-Net-based framework
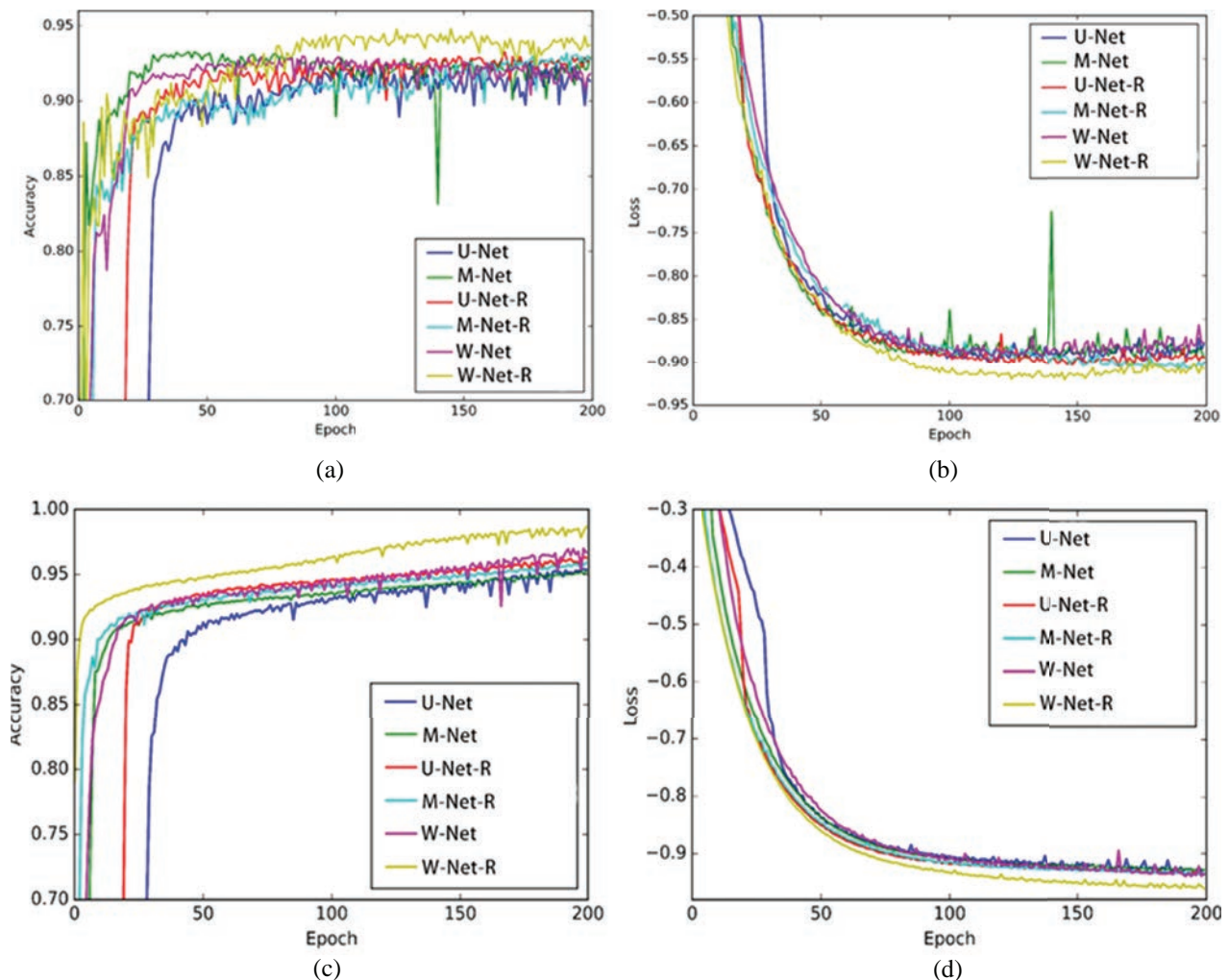
Fig. 3. Parameter changes during training and verification. (a) Accuracy of train set. (b) Loss function of train dataset. (c) Accuracy of verification dataset. (d) Loss function of verification dataset.
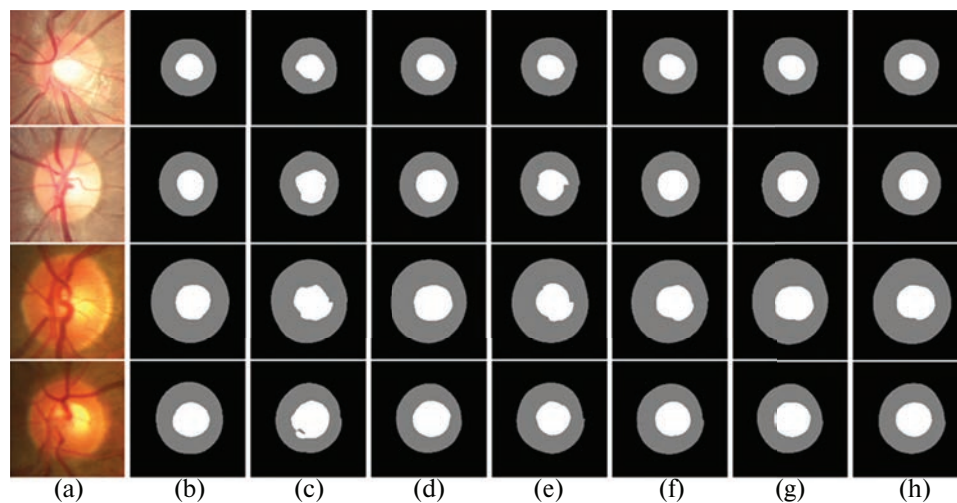
Fig. 4. Comparison of different network model. (a) Original image. (b) Label. (c) U-Net. (d) M-Net. (e) U-Net-R. (f) M-Net-R. (g) W-Net. (h) W-Net-R.

using common convolution unit (W-Net) and residual multi-scale convolution (W-Net-R), respectively. By calculating 5 evaluation metrics for OC and OD, the proposed W-Net-R is evaluated appropriately.

Table I shows the comparative results among 6 models for hybrid segmentation of OC and OD. The table demonstrated that the W-Net-R is superior to other networks on all the 5 evaluation metrics.

From the pairwise comparison of Table I, it can be seen that, under the same network framework, the performance of using the multiscale convolution module with residuals is significantly higher than that of ordinary modules. That is because, on one hand, multi-scale convolution of residuals uses receptive fields of different scales to obtain features of distinct levels, and thus enrich the semantic information. On the other hand, feature maps of different scales are connected for feature fusion, and residual learning with skip connections makes the network easier to train, effectively suppresses the problems of gradient disappearance and network degradation. Therefore, though W-Net-R deepened the network, its performance is not degraded.

Figure 3 shows the accuracy and loss function in the optimization process. Figures 3(a)–(b) denote the changes in accuracy and loss function on the training set; Figures 3(c)–(d) denote the changes in accuracy and loss function on the validating dataset. It is shown that W-Net-R is significantly higher in accuracy than other networks, meanwhile, its loss function can quickly converge and obtain the optimal.

As can be seen from Figure 3, comparing with other networks, on the accuracy, our proposed approach is slightly higher than other networks, meanwhile its loss function converge to obtain the best, which proves that the proposed method has stronger fitting ability and better feature extraction ability on the training dataset. While a high accuracy on the validating dataset indicates that our proposed method does not cause overfitting on the training set due to over-learning. It is proved that the proposed method has good generalization and robustness, and can learn strong distinctive representation from semantic information. Meanwhile, the high accuracy on the validating dataset indicates that the network has not over-trained the training set and caused over-fitting. The method has strong generalization and robustness, and can learn strong separability representation in image

semantic information. So that the network has better segmentation performance.

For proving the ability of generalization and robustness of our suggested framework, fundus images with different optical properties were chosen for demonstrations. As shown in Figure 4, the first two rows are from Zeiss Visucam 500 fundus camera, while the last two rows are from Canon CR-2 fundus camera. It is shown that the segmentation result by the W-Net-R model is closer to the expert's ground truth, with fewer noises and smoother edges, which is in accordance with results of Table I. In addition, a high accuracy of validation set in Figure 3(c) indicates that the proposed model does not cause overfitting due to over-learning. Therefore, the proposed method can achieve accurate performances on OC and OD when processing different kinds of fundus images with high/low contrast, and proves good generalization ability and robustness.

4. CONCLUSION

In this research, a residual multi-scale FCN framework named W-Net-R is proposed. The hybrid segmentation of OC and OD is taken for single-stage multi-label labeling problems. In the preprocessing stage, polar coordinate transformation was introduced for space constraining and CDR balancing. The proposed W-Net-R frame adds an image pyramid to the network to build the multi-scale inputting layer. In addition, multi-scale full convolution module with residuals makes full use of receptive fields of different sizes to extract different levels of semantic information. Moreover, combined with different levels of skip connections, the proposed method achieved feature reuse, feature propagation, and feature fusion at different depths. Meanwhile, the multi-label cost function is utilized for guiding the functioning of network. The Experiment results proved that comparing with current state-of-the-art models, our improved framework can increase the segmentation accuracy of OD and OC effectively, and shows good prospects in large-scale early screening of glaucoma. Due to the limitation of the study, on the segmentation accuracy OC and OD is concerned in this paper, and does not involve the evaluation of glaucoma screening (e.g., CDR).

In future research, we would focus on improving the accuracy and robustness of our proposed framework, and evaluate it via

more benchmark datasets. (e.g., ORIGA [24] and RIGA [25]). Moreover, the hyper-parameters in this paper are mainly manually selected based on experience and experimental results. Therefore, how to give a systematic approach for hyper-parameter adjustment is also a research direction of our future work.

Informed Consent

Informed consent was obtained from all patients for being included in the study.

Conflict of Interest

The authors declare that there is no conflict of interest in this study.

References and Notes

1. Tham, Y.C., Li, X., Wong, T.Y., Quigley, H.A., Aung, T. and Cheng, C.Y., **2014**. Global prevalence of glaucoma and projections of glaucoma burden through 2040: A systematic review and meta-analysis. *Ophthalmology, 121*(11), pp.2081–2090.
2. Garway-Heath, D.F. and Hitchings, R.A., **1998**. Quantitative evaluation of the optic nerve head in early glaucoma. *British Journal of Ophthalmology, 82*(4), pp.352–361.
3. Joshi, G.D., Sivaswamy, J. and Krishnadas, S.R., **2011**. Optic disk and cup segmentation from monocular color retinal images for glaucoma assessment. *IEEE Transactions on Medical Imaging, 30*(6), pp.1192–1205.
4. Dehghani, A., Moghaddam, H.A. and Moin, M.S., **2012**. Optic disc localization in retinal images using histogram matching. *EURASIP Journal on Image and Video Processing, 2012*(1), p.19.
5. Almazroa, A., Burman, R., Raahemifar, K. and Lakshminarayanan, V., **2015**. Optic disc and optic cup segmentation methodologies for glaucoma image detection: A survey. *Journal of Ophthalmology, 2015*.
6. Zheng, Y., Stambolian, D., O'Brien, J. and Gee, J.C., **2013**. Optic Disc and Cup Segmentation from Color Fundus Photograph Using Graph Cut with Priors. *International Conference on Medical Image Computing and Computer-Assisted Intervention,* September 22; Nagoya, Japan.
7. Aquino, A., Gegúndez-Arias, M.E. and Marín, D., **2010**. Detecting the optic disc boundary in digital fundus images using morphological, edge detection, and feature extraction techniques. *IEEE Transactions on Medical Imaging 29*(11), pp.1860–1869.
8. Cheng, J., Liu, J., Xu, Y.W., Yin, F.S., Damon, W.K.W., Tan, N.M., Tao, D.C., Cheng, C.Y., Aung, T. and Wong, T.Y., **2013**. Superpixel classification based optic disc and optic cup segmentation for glaucoma screening. *IEEE Transactions on Medical Imaging, 32*(6), pp.1019–1032.
9. Kamnitsas, K., Ledig, C., Newcombe, V.F., Simpson, J.P., Kane, A.D., Menon, D.K., Rueckert, D. and Glocker, B., **2017**. Efficient multi-scale 3D CNN with fully connected CRF for accurate brain lesion segmentation. *Medical Image Analysis, 36*(2017), pp.61–78.
10. Song, J., Yang, C., Fan, L., Wang, K., Yang, F., Liu, S. and Tian, J., **2015**. Lung lesion extraction using a toboggan based growing automatic segmentation approach. *IEEE Transactions on Medical Imaging, 35*(1), pp.337–353.
11. Ronneberger, O., Fischer, P. and Brox, T., **2015**. U-net: Convolutional Networks for Biomedical Image Segmentation. *International Conference on Medical Image Computing and Computer-Assisted Intervention,* October 5; Munich, Germany.
12. Fu, H., Cheng, J., Xu, Y., Wong, D.W.K., Liu, J. and Cao, X., **2018**. Joint optic disc and cup segmentation based on multi-label deep network and polar transformation. *IEEE Transactions on Medical Imaging, 37*(7), pp.1597–1605.
13. Zhou, Z., Siddiquee, M.M.R., Tajbakhsh, N. and Liang, J., **2018**. Unet++: A Nested U-net Architecture for Medical Image Segmentation. *Deep Learning in Medical Image Analysis and Multimodal Learning for Clinical Decision Support,* September 20; Granada, Spain. pp.3–11.
14. Ibtehaz, N. and Rahman, M.S., **2020**. MultiResUNet: Rethinking the U-Net architecture for multimodal biomedical image segmentation. *Neural Networks, 121*(2020), pp.74–87.
15. Dunnhofer, M., Antico, M., Sasazawa, F., Takeda, Y., Camps, S., Martinel, N., Micheloni, C., Carneiro, G. and Fontanarosa, D., **2020**. Siam-U-Net: Encoder-decoder siamese network for knee cartilage tracking in ultrasound images. *Medical Image Analysis, 60*(2020), p.101631.
16. Sevastopolsky, A., **2017**. Optic disc and cup segmentation methods for glaucoma detection with modification of U-Net convolutional neural network. *Pattern Recognition and Image Analysis, 27*(3), pp.618–624.
17. Aganj, I., Harisinghani, M.G., Weissleder, R. and Fischl, B., **2018**. Unsupervised medical image segmentation based on the local center of mass. *Scientific Reports, 8*(1), pp.1–8.
18. Ma, J., Fan, X., Yang, S.X., Zhang, X. and Zhu, X., **2018**. Contrast limited adaptive histogram equalization-based fusion in YIQ and HSI color spaces for underwater image enhancement. *International Journal of Pattern Recognition and Artificial Intelligence, 32*(7), p.1854018.
19. Crum, W.R., Camara, O. and Hill, D.L., **2006**. Generalized overlap measures for evaluation and validation in medical image analysis. *IEEE Transactions on Medical Imaging, 25*(11), pp.1451–1461.
20. Lin, T.Y., Goyal, P., Girshick, R., He, K. and Dollár, P., **2017**. Focal Loss for Dense Object Detection. *Proceedings of the IEEE International Conference on Computer Vision,* October 22; Venice, Italy.
21. Szegedy, C., Ioffe, S., Vanhoucke, V. and Alemi, A.A., **2017**. Inception-v4, Inception-Resnet and the Impact of Residual Connections on Learning. *Thirty-first AAAI Conference on Artificial Intelligence,* February 4; San Francisco, USA.
22. He, K., Zhang, X., Ren, S. and Sun, J., **2016**. Deep Residual Learning for Image Recognition. *Proceedings of the IEEE Conference on Computer Vision and Pattern Recognition,* June 26; Las Vegas, USA.
23. Gu, Z., Cheng, J., Fu, H., Zhou, K., Hao, H., Zhao, Y., Zhang, T.Y., Gao, S.H. and Liu, J., **2019**. CE-Net: Context encoder network for 2D medical image segmentation. *IEEE Transactions on Medical Imaging, 38*(10), pp.2281–2292.
24. Zhang, Z., Yin, F.S., Liu, J., Wong, W.K., Tan, N.M., Lee, B.H., Cheng, J. and Wong, T.Y., **2010**. Origa-Light: An Online Retinal Fundus Image Database for Glaucoma Analysis and Research. *2010 Annual International Conference of the IEEE Engineering in Medicine and Biology,* August 31; Buenos Aires, Argentina.
25. Almazroa, A., Alodhayb, S., Osman, E., Ramadan, E., Hummadi, M., Dlaim, M., Alkatee, M., Raahemifar, K. and Lakshminarayanan, V., **2018**. Retinal Fundus Images for Glaucoma Analysis: The RIGA Dataset. *Medical Imaging, 2018: Imaging Informatics for Healthcare, Research, and Applications,* February 13; Houston, USA.